energies

MDPI

Article

Forces in Axial Flux Magnetic Gears with Integer and Fractional Gear Ratios

Janusz Kołodziej *, Marcin Kowol *, Piotr Mynarek *, Rafał Gabor * and Marian Łukaniszyn *

The Faculty of Electrical Engineering, Automatic Control and Informatics, Opole University of Technology, 45-758 Opole, Poland

* Correspondence: ja.kolodziej@po.edu.pl (J.K.); m.kowol@po.edu.pl (M.K.); p.mynarek@po.edu.pl (P.M.); r.gabor@po.edu.pl (R.G.); m.lukaniszyn@po.edu.pl (M.Ł.)

Abstract: This paper presents a comparison of two variants of an axial flux magnetic gear (AFMG), namely, with integer and fractional gear ratios. Based on calculations derived with the use of three-dimensional numerical models, the torque characteristics of the analyzed AFMGs are computed and verified on a physical model. The greatest emphasis is put on the detailed decomposition and analysis of local forces in modulator pole pieces (also used in the structural analysis) within the no-load and maximal load conditions. The authors also describe the unbalanced magnetic forces (UMF) in the axial and radial directions resulting from the construction of the considered AFMGs variants, and their possible effects in the context of the use of additive manufacturing (AM) in prototypes. The paper also proposes an effective method for limiting the axial strain by using the asymmetry of the air gaps, which slightly reduces the torque transmitted by AFMGs. Finally, a static strength analysis was presented that allows us to assess the effects of local forces in the form of modulator disc deformation for selected cases of air gap asymmetry.

Keywords: axial magnetic gear; local and global force; flywheel energy storage systems; additive manufacturing; structural analysis

Citation: Kołodziej, J.; Kowol, M.; Mynarek, P.; Gabor, R.; Łukaniszyn, M. Forces in Axial Flux Magnetic Gears with Integer and Fractional Gear Ratios. *Energies* **2021**, *14*, 855. https://doi.org/10.3390/en14040855

Academic Editors: Krzysztof Górecki and Mario Marchesoni

Received: 5 January 2021

Accepted: 2 February 2021

Published: 6 February 2021

1. Introduction

Current constructions of electromechanical transducers are mainly high-performance, rotating, energy conversion systems. In this respect, radial flux machines play a dominant role. This tendency is also observed for a family of magnetic gears (MGs), which is relatively young and, at the same time, very diverse in terms of their design. In fact, the advantages of contactless energy transmission/conversion using the magnetic field were discovered based on a concentric magnetic gear examined in the papers [1,2]. An alternative to mechanical gears, which are often noisy and require lubrication and maintenance, was thus developed. However, an important parameter in favor of traditional mechanical gears is their ability to transfer high torques. The assets of reduced power losses and resistance to the possible mechanical damage caused by overloads come to light in this, and favor magnetic gears.

However, modern applications, in particular in the automotive industry, require much more from electromechanical transducers. Limited installation space, aspects of design, or the application nature have directed researchers' attention towards axial flux (AF), and less often transverse flux (TF), electrical machines. The remarkably higher efficiency of the use of magnetic flux, in addition to the easier cooling in these systems, makes it possible to design structures with very high power density. The appearance of a study [3] on a group of AFMGs was only a matter of time. This subject has been continued in papers [4–11], wherein a number of analyses concerning the principles of operation and the design aspects of these gears, largely supported by measurements, were presented. Given the nature of the phenomena in the mentioned group of MGs, the majority of the papers employ 3D numerical models; however, the authors of Ref. [4] also indicate the possibility of applying 2D analytical models. Comparative analyses of radial flux MGs (RFMGs), as well as new AF

and TF MG solutions, demonstrated in the papers [7–9] point to the numerous advantages and potential uses of the new MG topologies. The issue discussed in the paper [9] is still topical, and concerns the aspect of selecting the topology and type of the permanent magnets so that the manufacturing costs of such gears are reduced. The paper [10] presents the advantages, which include a significant increase in torque density with a simultaneous pulsation reduction resulting from the use of the Halbach magnetization.

All of these works [3–12] are consistent when it comes to the limitations caused by axial forces. They point to the need to reduce axial forces and to ensure appropriate gear rigidity as early as at the design phase, also taking the bearing arrangement into account. An increase in the torque is closely related to an increase in axial forces. The easiest way to reduce this adverse effect is to increase the air gap thickness [5]; however, this operation reduces the transmitted torque as well. A detailed analysis of AFMGs included in the paper [6] demonstrates that it is possible to design a structure with relatively low axial forces and high torque density by means of parameterized numerical calculations. Additionally, an interesting analysis of unbalanced axial force and their minimization, using an additional rotor, was presented in the papers [13–15], with regard to a cycloidal magnetic gear. The analysis of radial and axial forces, with reference to electric machines (both with radial and axial structures) containing permanent magnets, is also undertaken in the works [16–18].

A relatively small number of works concern the issue of MG's structural analysis, and in particular its crucial element—the modulator [19,20]. Ensuring the adequate rigidity of gear parts is a particularly relevant issue at the prototyping phase, using tools and additive methods, while this is not a significant problem for MGs with relatively short active length and low radial forces [21]. As shown in Ref. [11], the use of additive manufacturing (AM) for the topology of MGs with axial forces and a torque density of 70kN/m^3 may be very difficult or even impossible. Therefore, the main objective of this paper is to fill the knowledge gap by analyzing local interactions within modulator cores in terms of the rigidity of the entire AFMG modulator structure. While considering two AFMG configurations with integer (G_{r1} = 5:1) and fractional (G_{r2} = 5.5:1) gear ratios, the authors also wish to consider the radial unbalanced magnetic forces (RUMF) derived from RFMGs [21]. In this paper, we focus on a detailed decomposition of local forces and the analysis of their components in terms of magnetic pull reduction, pulsation reduction and modulator rigidity, keeping the total air gaps' thickness constant; these being challenging issues not yet deeply considered.

This paper is structured as follows. Having introduced in Section 1 the problem of forces acting in AFMGs, a prototype construction of an AFPM with a much more advantageous fractional gear ratio is presented in Section 2. The magnetic field analysis, torque calculation and validation in Section 3 clearly confirm the advantages of the AFMG's configuration with a fractional gear ratio. The most important section, Section 4, provides a detailed analysis of forces in AFMGs, including the locked low-speed rotor and modulator, normal synchronous operation, and finally, a new method for axial-force reduction. The structural analysis tools of Section 5 aim to assess a favorable use of additive manufacturing in the construction of AFMGs. The conclusion of Section 6 completes the paper.

2. Physical Model

The main advantage of axial flux gears is their characteristic disc-shaped design. Their low active length, as compared to their diameter, allows them to be installed in hard-to-reach and limited spaces. For AFMGs, if the radius increases, volumetric torque density (VTD) increases much faster, with a similar value of PM gravimetric torque density (PM GTD) as compared to RFMGs [10]. In addition to these indicators, the possibility/susceptibility of building multi-level structures, the easier hermetic sealing of elements due to the arrangement of flat discs, and the relatively low sensitivity to air gap width were also noticed in the context of the application of flywheel energy storage systems (FESS) [12]. Undoubtedly, the potential of using AFMGs in contactless charging systems for public

transport vehicles is a perfect addition to the modern trends of progressing urbanization combined with environmental protection, in terms of clean air.

The authors of this paper have been researching MGs for some time [21–23]; however, their main focus so far has been on coaxial MGs (CMGs, being also part of an RFMG). Taking into account the principle of operation of CMGs and AFMGs, the selection of rotor pole pairs (high- and low-speed rotors—p_h, p_l) and ferromagnetic pole pieces (n_s) is identical. Using their experience and measurement facilities, the authors of this paper focus on two AFMG variants with a combination of $p_h/n_s/p_l$. For the first variant—MG_1—a combination of 2/10/8 was used for a locked low-speed rotor to obtain a gear ratio of $G_{R1} = 1 + p_l/p_h = 5$, while for the other variant—MG_2—a combination of 2/11/9 gave a gear ratio of $G_{R2} = 5.5$. Except for the spans and number of modulator ferromagnetic cores and low-speed rotor permanent magnets, all relevant geometric parameters of the analyzed AFMGs variants were the same and are given in Table 1.

Table 1. Design parameters for the axial-flux magnetic gears.

Geometric Parameters	mm
Back iron outer radios (R_{BI})	75
Back iron thickness (T_{BI})	5
High- and low-speed rotor PMs inner radius (R_1)	40
High- and low-speed rotor PMs outer radius (R_2)	70
High- and low-speed rotor PMs thickness (T_{PMs})	10
Modulator pole pieces inner radius (R_3)	40
Modulator pole pieces outer radius (R_4)	70
Modulator pole pieces thickness (T_{PP})	10
Air gaps thickness (T_{AG})	2.5

The selection of structures with integer and fractional gear ratios is intentional, and dictated by the desire to present a comparative analysis of the distribution of axial forces and stresses characteristic of AFMGs, and radial unbalanced magnetic forces (RUMF) characteristic of RFMGs, with a fractional gear ratio and gcd < 2. To date, a relatively low number of publications have provided a detailed discussion about the effects of local forces acting on AFMG modulator cores, in the context of the rigidity of the entire element and the possible reduction of global magnetic forces.

It is well known that the selection of materials used in MGs cannot be left to chance. Despite there being no visible differences in the calculated values of torque in the static analysis, magnetic field fluctuations caused by the movement of gear elements may lead to large power losses and a reduction in the key parameter, which is efficiency. An effective way to eliminate/reduce them is to use lamination or soft magnetic composites (SMCs), as shown in the paper [22]. However, the specific design of AFMGs makes it difficult to apply lamination due to the need to ensure structural rigidity and install permanent magnets. Therefore, in the MG_2 prototype shown in Figure 1, the authors decided to make the yokes of both rotors from solid steel, despite higher power losses. Soft magnetic composites (Somaloy 700) were used to build the modulator. Individual modulator cores were positioned in relation to the rotors using structural elements made through additive manufacturing methods. All active elements were centered on the shaft made of acid-resistant steel, using a double arrangement of double-row bearings.

Summarizing the prototype construction section, it is worth emphasizing that on the basis of a literature review and our simulation and experimental experiences, we have decided to build a much more advantageous MG_2 prototype (rather than MG_1). This physical model will be used in the validation of both integer/simulation and fractional/experimental variants of AFMGs in the next section.

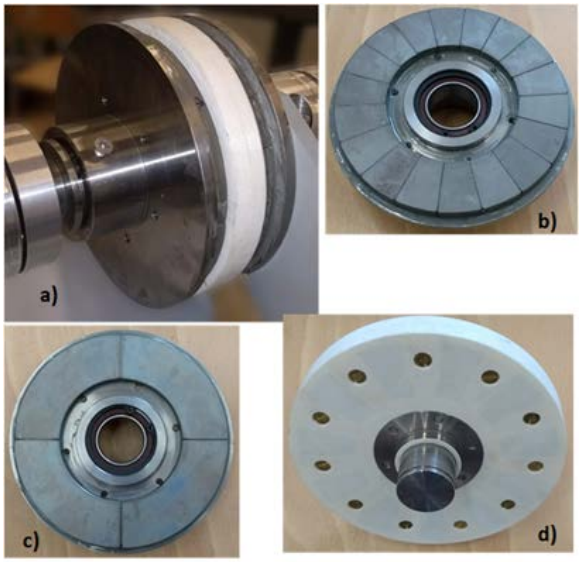

Figure 1. (**a**) AFMG prototype (MG_2: 2/11/9 G_{R2} = 5.5), (**b**,**c**) low- and high-speed rotors, respectively, (**d**) made using additive technology modulator containing SMC cores.

3. Magnetic Field Analysis, Torque Calculations and Validation

The seemingly simple issue of the static analysis of the magnetic field in MGs often involves two-dimensional numerical analysis only. A detailed analysis of end-effects (leakage, fringing, and escaping) presented in the papers [10,24] clearly points to the need to be rather careful when designing RFMGs, which are theoretically simpler to describe. In the majority of cases, the nature of the magnetic field characteristic of axial flux machines and the requirements for calculation accuracy necessitate the use of three-dimensional numerical models. The vector distribution of the magnetic field for the selected cross-sectional plane of the MG_2 model shown in Figure 2 illustrates its complexity and potential sensitivity to fringing. The plane is oriented such that it passes through the center of the core (pole piece) and into the opposite side of the air area. The visible high densities of vectors in the MG central and external areas suggest possible fringing areas. However, the detailed analysis of this magnetic field distribution, which also considers the modulus of individual vectors, suggests that magnetic field fringing is relatively low. Still, it seems advisable to use a material with low magnetic permeability for the shaft and external covers. It is also difficult to provide a definite answer in terms of the advantage of an axial flux gear over a radial flux one.

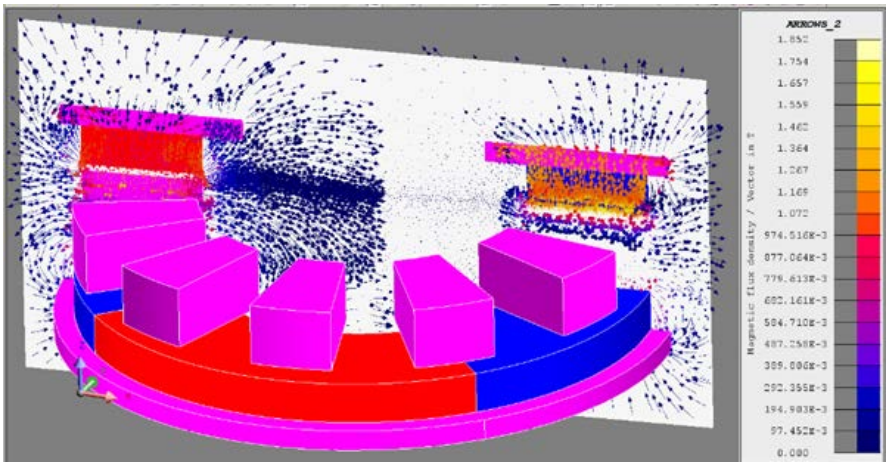

Figure 2. Magnetic field of AFMG (MG_2: 2/11/9 G_{R2} = 5.5).

A factor that significantly hinders the detailed analysis of the magnetic field, especially for AFMGs with a fractional gear ratio, is the large number of calculations related to the need to perform calculations for the entire model. When designing a gear for a specific application, it seems valuable to use simplified analytical models during preliminary analyses [4], as they make it possible to select key geometric parameters. However, the main objective of this paper is to analyze the spatial distribution of magnetic forces in detail, including local effects, which determines the use of three-dimensional magnetic field analysis tools.

Despite their very similar designs, the AFMG models considered in the paper differ in one relevant aspect, which is the gear ratio. In spite of a relatively small difference in the mentioned gear ratio, significant changes in the torque characteristics (Figure 3a) are observed, which are also mentioned by other authors [12,24]. An over fourfold increase in magnetic torque pulsation for MG_1 significantly affects the ergonomics of the gear, which is magnetically balanced in theory. The lines visible on the FFT spectral torque characteristics (Figure 3c,d) and the determined total harmonic distortion (THD) values point to a clear advantage of the structure with a fractional gear ratio. Even though the paper focuses on two AFMG configurations, the authors decided to verify only one of them through measurements. Detailed measurements of static characteristics were performed for the MG_2 gear with a fractional gear ratio. Figure 3b presents the obtained results of torques associated with the high-speed rotor and the modulator. In our opinion, the discrepancies visible in the presented characteristics are acceptable and allow for a further simulation-based discussion.

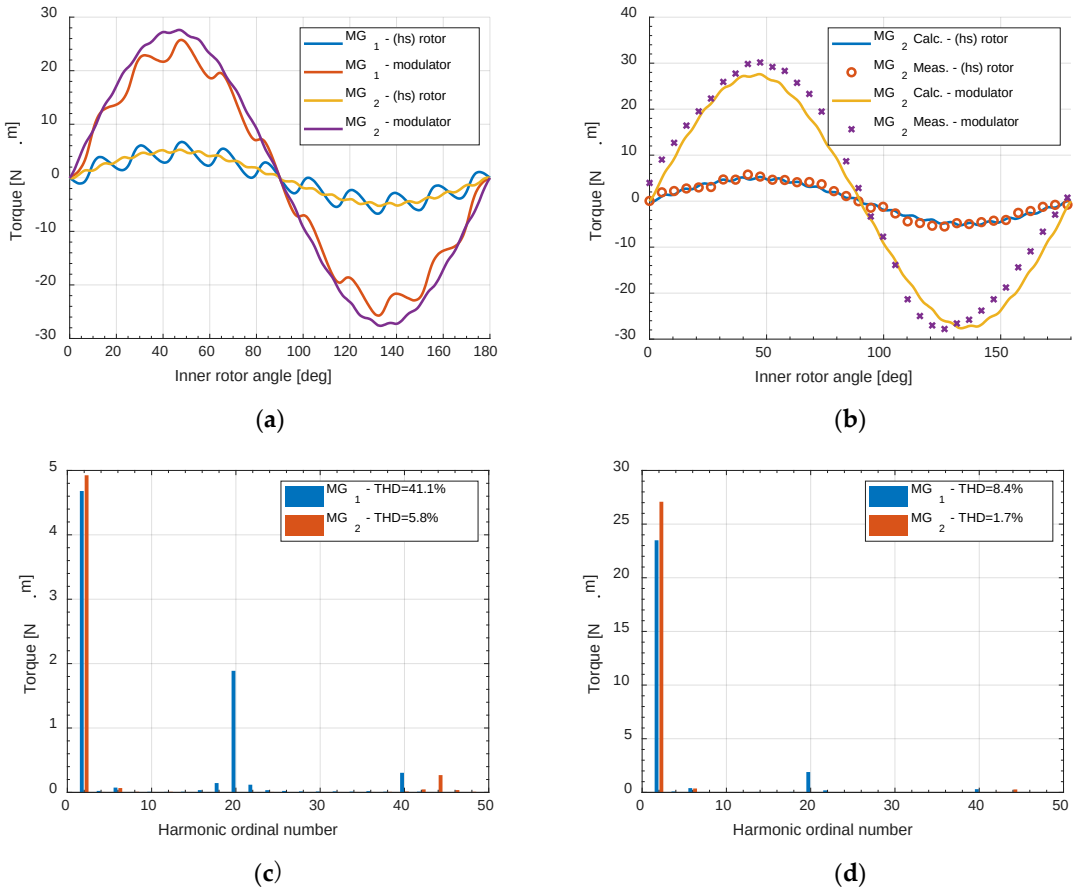

Figure 3. (**a**) Calculated torque characteristics for AFMGs with ratios 5:1 and 5.5:1, (**b**) comparison of calculations with measurements for MG_2, (**c**,**d**) FFT spectra for high-speed (hs) rotor and modulator torque, respectively.

4. Force Analysis in AFMGs

4.1. Locked Low-Speed Rotor and Modulator

In practically every publication concerning AFMGs, the authors point to the occurrence of axial forces resulting in the necessity to ensure the appropriate rigidity of the rotating elements. With the focus placed on axial forces, other local effects are omitted, which affects output torque characteristics, torque pulsations, and, in some cases, radial unbalanced magnetic forces (RUMF). While the authors came across papers about these issues in RFMGs [21,25,26] during the literature review, they did not find any papers about these issues in AFMGs.

The two gear variants selected for analysis in this paper operate in a configuration with a locked low-speed rotor. Still, the element that is potentially exposed to the highest forces in the gear is the modulator. In the introduction to force analysis, the authors focus on the evaluation of effects near/in the area of the locked modulator cores. The locked output element makes it possible to omit centrifugal forces in the analysis but requires all cores to be described. In this case, it is also necessary to introduce the numbering of the cores and the related unambiguous orientation of their local coordinate system, as shown in Figure 4. The local forces acting on each core $\vec{F}_{P_i}$ were described using three components, F_{rP_i}, $F_{\vartheta P_i}$, F_{zP_i}, in accordance with the arrangement of unit vectors marked in Figure 4c.

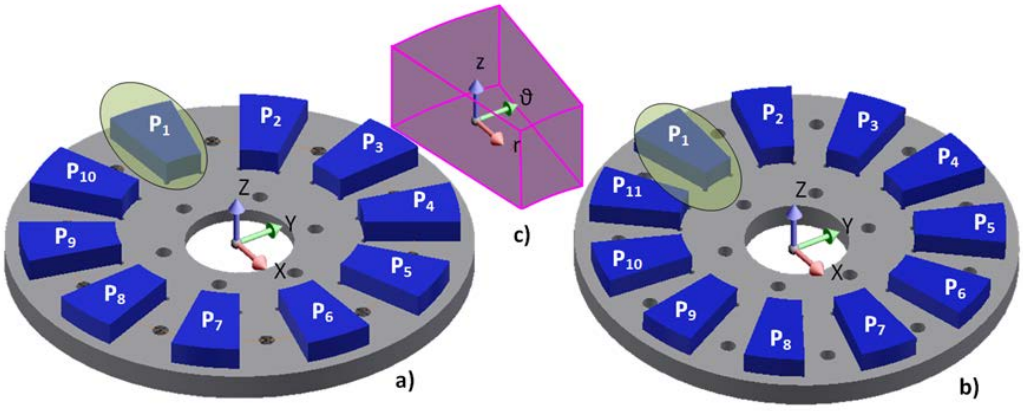

Figure 4. (**a**,**b**) Pole pieces numbering for MG_1 and MG_2, respectively; (**c**) local coordinate system assigned to any core.

Due to the very similar designs of the gear variants (MG_1 and MG_2) analyzed, the calculations of the distribution of local forces for individual modulator cores were also very similar in the obtained characteristics. The main difference only includes the span of the characteristics resulting from a different number of pole pairs and the holistic combinations presented later in this paper. With this in mind, the authors present only a detailed distribution of the components of local forces for the MG_2 gear variant. The variability in the force acting on the selected core shown in Figure 5 reveals that the largest differences characterize components $F_{\vartheta P1}$, F_{zP1}; in addition, the sense of these components changes.

Component F_{rP1} fluctuates the least, while maintaining its applicability to the system rotation axis. However, the specific nature of the gear operating state, i.e., with the modulator locked, means that each core is affected by different interactions due to the angular position of the perimeter. With this in mind, Figure 5b–d shows the angular variability of these components, including all cores from P_1 to P_{11}. Based on the analysis of the envelopes of the obtained characteristics, it can be seen that the radial forces are by far the smallest and always face the gear rotation axis. Considering the tangent and axial components, differences between individual cores in terms of both value and nature can be easily noticed.

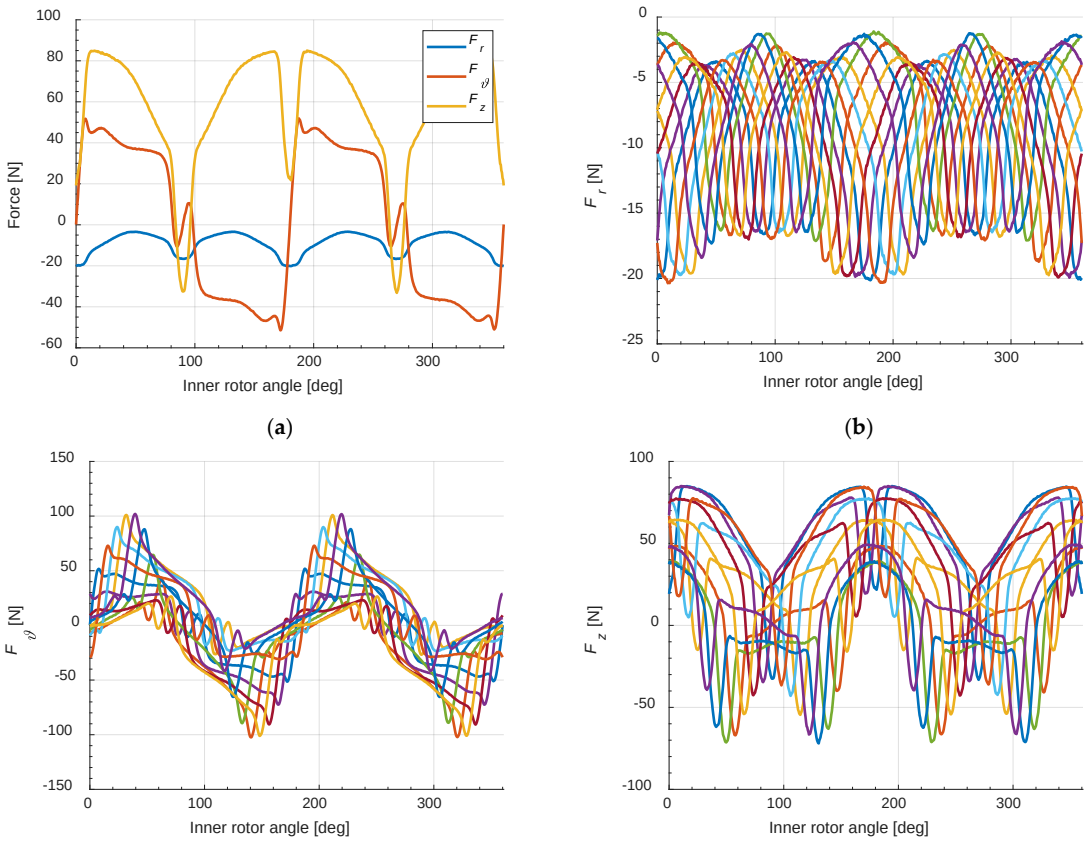

Figure 5. Local forces components (F_r, F_ϑ, F_z,) of MG_2 (**a**) in reference to single pole piece no. P_1, (**b**–**d**) for all cores P_1–P_{11}.

The analysis of magnetic forces in radial and axial directions is also interesting. Treating the modulator as a rigid element, the geometric summation of local force components was performed. Equations (1) and (2) describe the resultant radial F_{rTot} and axial F_{zTot} force, respectively. The calculations also involved checking the torque value T_{mid} using Equation (3). Figure 6 shows the resultant forces depending on the angle of rotation of the high-speed rotor (α_{in}). The magnetic unbalance caused by a fractional gear ratio for the MG_2 variant (Figure 6a) is marginal compared to the axial force seen in both MG designs (Figure 6b):

$$F_{rTot}(\alpha_{in}) = \sum_{i=1}^{n_s} F_{rP_i}(\alpha_{in}) \tag{1}$$

$$F_{zTot}(\alpha_{in}) = \sum_{i=1}^{n_s} F_{zP_i}(\alpha_{in}) \tag{2}$$

$$T_{mid} = \left(\sum_{i=1}^{n_s} F_{\vartheta P_i} \right) r_{mid} \tag{3}$$

4.2. Normal Synchronous Operating

Magnetic gears belong to a group of synchronous machines. In normal operation, for loads not exceeding the limit values, the powered high-speed rotor, rotating at a certain speed, simultaneously forces the modulator to rotate according to the gear ratio. The assumed maximum modulator speed is 500 rpm, which, in extreme cases, translates into a centrifugal force of approx. 16 N. Each modulator core is also subject to identical and cyclically changing loads, which result from the magnetic geometry of the gear. On this basis, the analysis of local magnetic effects was limited to one core for each gear variant

under consideration, taking into account two extreme operating states, which were no load (Figure 7) and maximum load (Figure 8). For all analyzed cases, it was observed that the sense of the resultant radial force F_r always faces the gear axis. Despite its relatively small amplitude, it has a compensatory effect on centrifugal forces (and is associated with the fact that the magnetic system approaches geometric and magnetic stability), which can be particularly important for higher speeds.

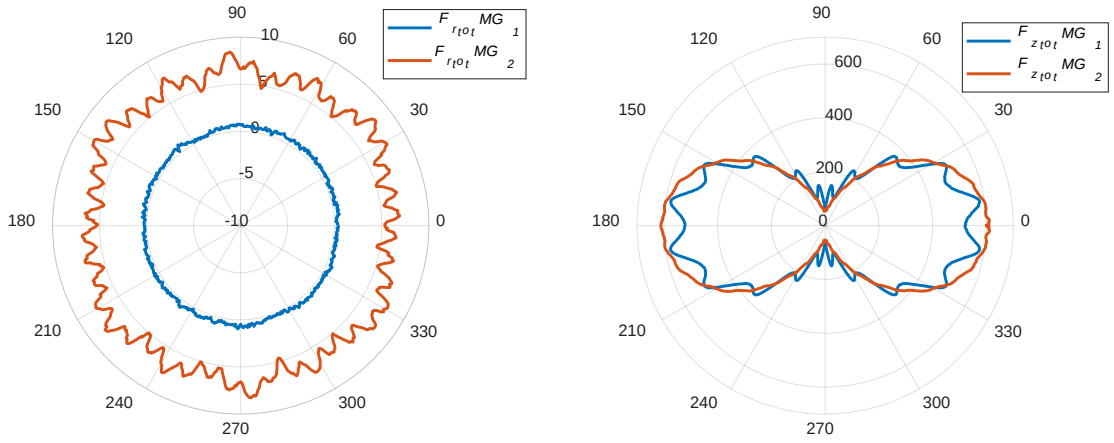

(**a**) (**b**)

Figure 6. Comparison of RUMF (**a**) and AUMF (**b**) for the two gear variants vs. high-speed rotor angle position, by fixed low-speed rotor and modulator.

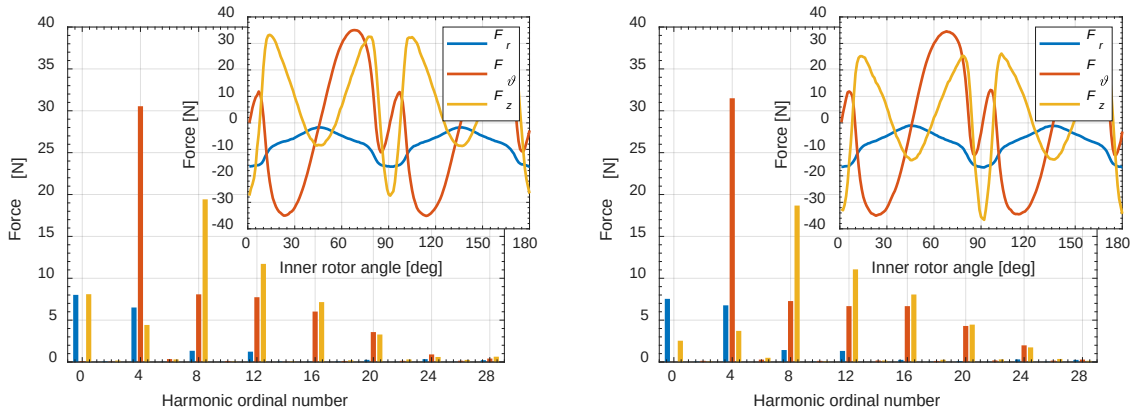

(**a**) (**b**)

Figure 7. Force components acting on a selected SMC modulator core and their FFT spectra at no load for two gear variants: (**a**) MG_1 (**b**) MG_2.

In the idle state (Figure 7a,b), for both MG variants, the tangent component F_ϑ is subject to the highest fluctuations, while the clearly dominant 4th harmonic is associated with the number of high-speed rotor pole pairs. For loaded gears (Figure 8a,b), the appearance of a constant component in the tangential force component spectrum responsible for torque transfer can be seen, which was to be expected. Small discrepancies in the spectrum of component F_z in the idle state are mainly due to the differences in the number and angular span of the modulator cores and low-speed rotor magnets in both gear variants. Under maximum load, the value of the constant component and the 4th harmonic increases considerably, which is the system's response to the extension of the core away from the neutral axis caused by the load. Although local, because it is limited to a single core, the analysis presented in this paper provides some relevant information that is useful for possible vibroacoustic, strength and ageing tests, especially in terms of prototyping

using additive manufacturing methods. However, the synthesis of local effects is also an interesting issue, as it allows the properties of the MG variants under consideration to be assessed as a whole.

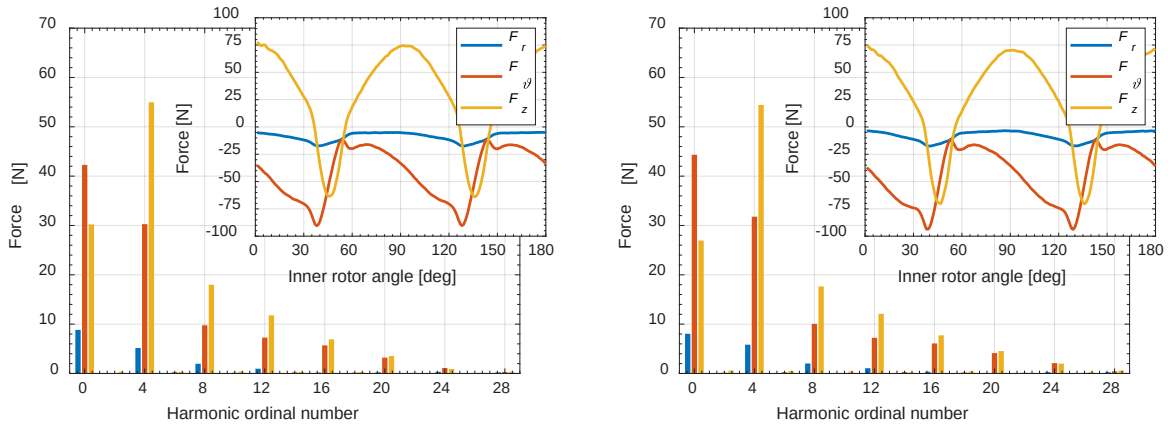

Figure 8. Force components acting on a selected SMC modulator core and their FFT spectra at max. load for two gear variants: (**a**) MG_1 (**b**) MG_2.

It is well-known that there are numerous limitations on designing MGs. The symmetrization of the magnetic circuit may also lead to a worse performance. The resultants—the total components of the force acting on the rigid modulator body—shown in Figure 9a,b are a perfect example of this effect. For the gear with a total gear ratio (MG_1), there are high fluctuations of components $F_{\vartheta Tot}$ and F_{zTot} in both idle and maximum load states. However, MG_2 is characterized by much lower variability in this respect. A slightly higher value of component $F_{\vartheta Tot}$ for the gear with a fractional gear ratio goes hand in hand with the much lower pulsation. Unfortunately, for both variants under consideration (Figure 9a,b), a relatively large value of component F_{zTot} is observed. This is associated with the axial force whose sense faces the low-speed rotor. For the idle state of MG_1, a significantly higher mean value and pulsations of this component are observed. For the maximum load state, the mean values of the component F_{zTot} are similar and high, considerably overloading the bearing system in the axial direction. The analysis of torques in Section 3 also confirms the better operational properties of the second MG variant. The asymmetry of the MG_2 magnetic circuit resulting in a non-zero value of radial component F_{rTot} is marginal, and does not have a considerable effect on the mechanical system, that is, the bearings.

4.3. Axial Force Reduction Method

Despite significant structural differences, AFMGs and RFMGs have comparable parameters in many aspects. A relatively high ratio of the diameter to the active length, which is typical of AFMGs, offers advantages in terms of application, but also has some mechanical limitations. As also confirmed in the previous Section 4.2, the disadvantage is indicated in numerous works [3–11], which results from the existence of axial magnetic forces, and may constitute a significant design limitation. A remedy for this is to increase the air gap widths, which is a certain improvement when combined with the lower sensitivity of AF gears to this parameter as compared to RF gears. However, this always involves a reduction of the torque transferred. This Section is inspired by the paper [12], wherein the use of AFMGs for energy transfer in the context of FESS application was discussed. When analyzing the available literature, no detailed description of the methods for selecting the width of the air gap from the point of view of axial force and shaft load was found. In this part of the paper, the authors will attempt to present their own experiences and conclusions.

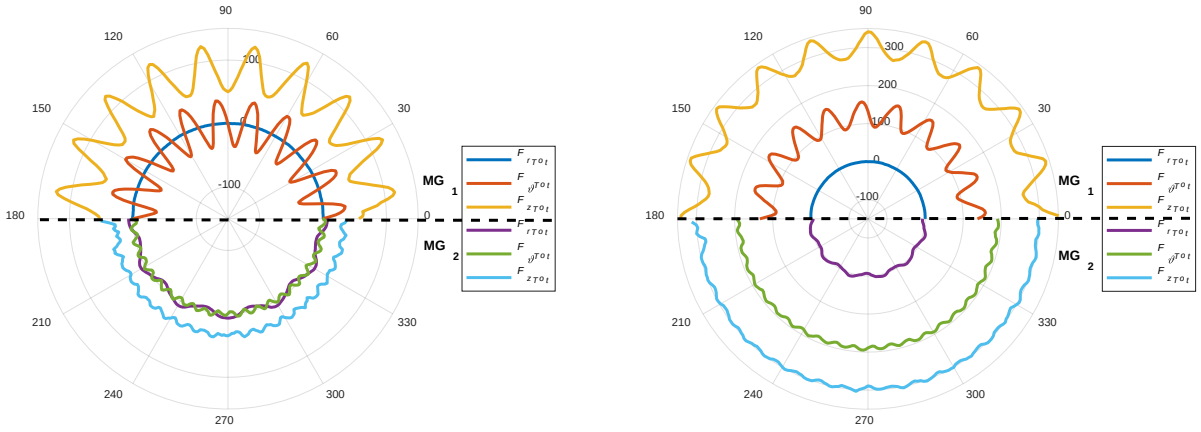

Figure 9. Global force components acting on the whole modulator vs. inner rotor angle, for two gear variants (upper chart part MG_1, lower chart part MG_2) at (**a**) no load and (**b**) max. load.

In the AFMG prototype presented in Section 2 of this paper, identical widths for both air gaps were employed (Table 1). This state was chosen as a starting point for further analysis, in which a simultaneous modification of air gaps between the modulator and the high-speed rotor (Ag_{high}) and low-speed rotor (Ag_{low}) was proposed according to Figure 10a. Even though the total (sum of) air gap width did not change, this modification led to a change in the value of the torque transferred.

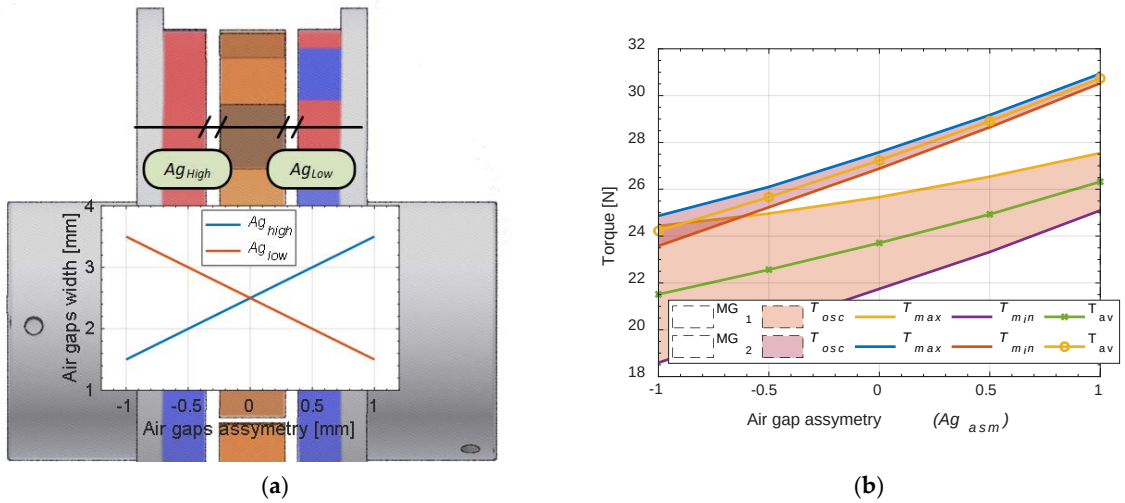

Figure 10. (**a**) The variants of the air gap asymmetry. (**b**) Calculated torque characteristics (T_{min}, T_{av}, T_{max}) for AFMGs (MG_1 and MG_2) vs. air gap asymmetry (Ag_{asm}).

The torque range (Figure 10b) resulting from the limit values assumed in the analysis is approx. 5 N·m (18.5%) for MG_1 and approx. 7 N·m (22.5%) for MG_2. It can therefore be concluded that these changes are significant. The area between the dotted lines describes the amplitude of the torque pulsations, which is related to the existence of higher harmonics in the spectral characteristic. Again, the much higher pulsations underline the considerably better operating parameters of the MG_2 gear with a fractional gear ratio. In addition, the area related to torque pulsations narrows considerably with a positive increase in the asymmetry of the air gaps.

Still, the analysis of local magnetic forces and their impact on the rigidity of the modulator made using additive manufacturing methods for the proposed variants in air

gap widths is considerably more interesting. These issues are discussed in the following Section of this paper. In a simplified analysis, it can be assumed that the modulator is not deformed, which allows local interactions to be considered as a whole. As in Section 4.1, using Equation (2), the authors in this part of the paper only focus on component F_{zTot} for the rigid modulator body. The analysis includes two MG operating states—no load and maximum load. The variability of component F_{zTot} as a function of the angle of rotation of the high-speed rotor for the selected five variants of air gap asymmetry and full load is given in Figure 11a. A noticeable increase in axial component pulsations with the negative asymmetry of air gaps ($Ag_{high} < Ag_{low}$) applies to both operating states and is particularly high for the MG_1 gear.

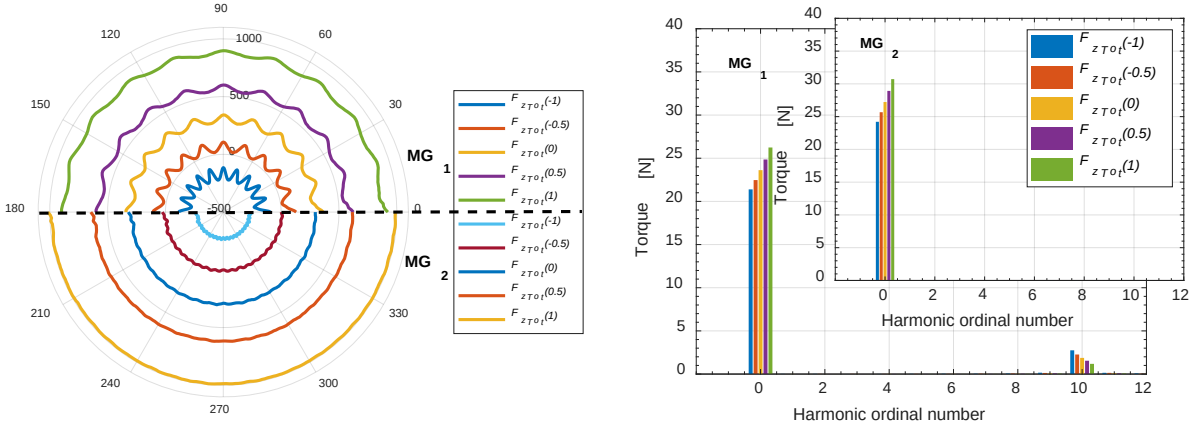

(**a**) (**b**)

Figure 11. Global force components acting on whole modulator vs. inner rotor angle and air gap asymmetry (Ag_{asm}), for the two gear variants (MG_1 and MG_2) at (**a**) max load; (**b**) FFT spectra of magnetic torque.

The value of the axial force is strongly dependent on the operating point, as illustrated by the characteristics shown in Figure 12. As shown on the characteristics, both gear variants are relatively well-balanced in the idle state, considering magnetic forces in the Z axis. However, moving to the rated load with the symmetry of the air gaps, as in the prototype, causes the axial load facing the low-speed rotor of approx. 300 N to appear. As is commonly accepted, in the extreme case, when analyzing the asymmetry variant $Ag_{asm} = +1$, the value of the axial force approaches 1 kN facing the low-speed rotor. When using the opposite asymmetry variant $Ag_{asm} = -1$, the axial force facing the high-speed rotor appears. As it is commonly accepted, electromechanical transducers are built for a given operating point. For the analyzed AFMGs operating under full load, the most advantageous air gap width variant in terms of balancing axial loads is $Ag_{asm} \approx -0.5$. In this configuration, the axial force was almost entirely eliminated; however, the torque was also reduced.

Detailed information on the effect of changing the air gap configuration is given in Table 2. A relatively small change to the air gap widths with a small reduction in torque (approx. 5%) results in an almost 80–100% reduction in axial forces. This is of particular importance when prototyping with the use of additive manufacturing methods, because the designer should be particularly careful due to the relatively low rigidity of plastic. However, the holistic approach to the distribution of magnetic forces presented in this Section is very simplified, and shows certain tendencies, but it cannot replace a complete strength analysis, which also includes local interactions.

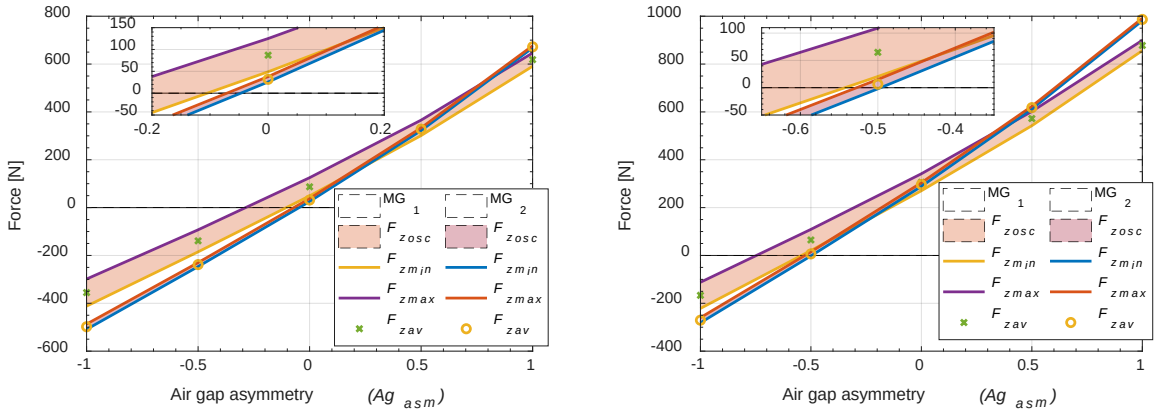

Figure 12. Global force F_{zTot} components acting on whole modulator vs. inner rotor angle and air gap asymmetry, for the two gear variants at (**a**) no load and (**b**) max load (MG_1 and MG_2).

Table 2. Design parameters for the axial flux magnetic gears.

AFMG	Air Gap Asymmetry Case	Torque		Force (F_{zTot})	
		Value (N·m)	Change (%)	Value (N)	Change (%)
	$Ag_{asm} = -0.5$	22.6	↓4.6	64	↓79
	$Ag_{asm} = 0$	23.7	---	304	---
	$Ag_{asm} = 1$	26.2	↑11	991	↑326
	$Ag_{asm} = -0.5$	25.7	↓5.7	6	↓98
	$Ag_{asm} = 0$ (prototype)	27.7	---	288	---
	$Ag_{asm} = 1$	30.7	↑11	877	↑305

5. Structural Analysis

The air gap asymmetry variant ($Ag_{asm} = -0.5$) presented in the previous Section almost eliminated the global axial force for the modulators of both magnetic gear variants, which are analyzed in this paper. However, the authors still expect rather high local interactions (Figure 8), which, due to the low stiffness of the elements made with the use of additive manufacturing methods, may cause significant deformation at some points. For this purpose, the CAD software was used to prepare appropriate models for the static simulation of stresses and deformations.

The no load state was omitted in the static strength analysis, so the authors focused only on the three air gap asymmetry variants given in Table 2 in the maximum load state for both gears. Considering the cyclic changes in the individual force components resulting from rotation, the least favorable angular positions causing the highest stresses and deformations were determined with the use of initial calculations. As shown in Figure 13a, the values of the individual components of the forces acting on each core were read for the selected operating point. Then, maintaining the appropriate numbering of the cores and the orientation of local coordinate systems (Figure 4), these data were entered into a mechanical model (Figure 13b). Except for printed components, the material properties of gear components were downloaded from a catalogue database, while the mechanical properties of the (3D) printed elements were determined with the use of the authors' own strength tests [21,27]. The analysis also included all auxiliary structural components, such as screws, etc., which ensures the mechanical integrity of the modulator. At the same time, boundary conditions blocking all degrees of freedom of the gear shaft were applied, with the analysis covering the modulator disc only.

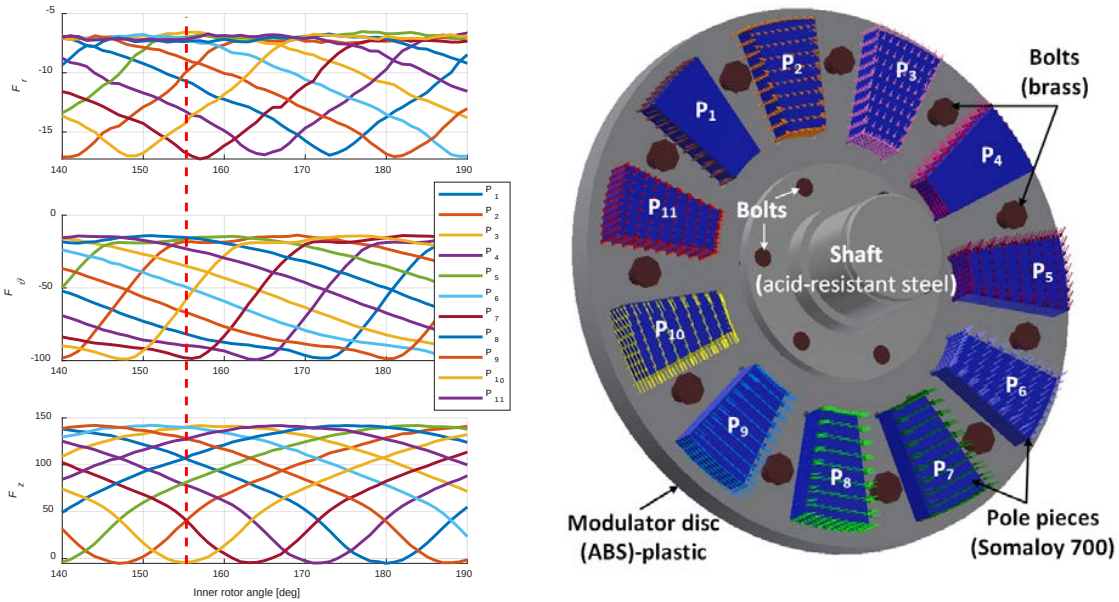

(**a**) (**b**)

Figure 13. (**a**) Forces components (F_r, F_ϑ, F_z,) of MG_2 for all modulator cores (P_1–P_{11}) used in the mechanical analysis, (**b**) part of modulator disc with visualization of forces applied to each of SMC cores.

However, the unambiguous evaluation of the results of the simulations mentioned above is hindered due to the differences in the gear ratios of the analyzed gears. The results obtained include deformations in all planes defined by the global coordinate system. However, the axial direction is critical from the point of view of gear design. As a result, the paper (Figure 14) only presents deformations in the Z direction, with deformations in the XY plane being omitted (despite being high). As expected, there is a clear correlation between the maximum torque and the level of deformation. Comparing the MG output models for identical air gaps (Ag_{asm} = 0), it can be seen that the MG_2 modulator is subject to considerably higher deformations, in an extreme case reaching approx. 130 µm; i.e., the value is approx. 35% higher than that for MG_1. Where does this difference come from? The key parameter must therefore be the torque of both gears; however, the difference here is approx. 15%. Therefore, the reason for this is a different distribution of forces attributed to the adjacent cores, which results from a different number of modulator cores. In addition, the magnetic symmetry of MG_1 is easily seen on the deformation map (Figure 14a,b), but it cannot be seen on the deformation maps for MG_2 (Figure 14d,e).

When assessing the modulator balanced in the Z axis (Ag_{asm} = −0.5), it can be clearly observed that the local interactions neutralize each other (Figure 14a,d). Despite large differences resulting from the design of the analyzed modulators, the detailed analysis of local interactions in this variant confirms the near-zero global axial imbalance value presented in Section 4.3 (Figure 12b). Different levels of absolute deformations for both gear variants mainly result from torque differences.

The extreme air gap asymmetry (Ag_{asm} = +1) shown in Figure 14c,f is characterized by the highest number of similarities in terms of stress and deformation distributions. A much higher effect of the low-speed rotor caused by a small air gap width results in an axial deformation that is almost evenly distributed along the outer modulator perimeter. When the modulator is deformed, its shape resembles a truncated cone. The observed extreme deformations of 200–300 µm, depending on the MG variant, amount to approx. 20–30% of the working gap width, which must have further consequences. Therefore, it can be concluded that the use of additive manufacturing methods to design a prototype of a modulator for these gear variants is unjustified, and can lead to potential rapid gear damage and, certainly, significant discrepancies between calculations and measurements.

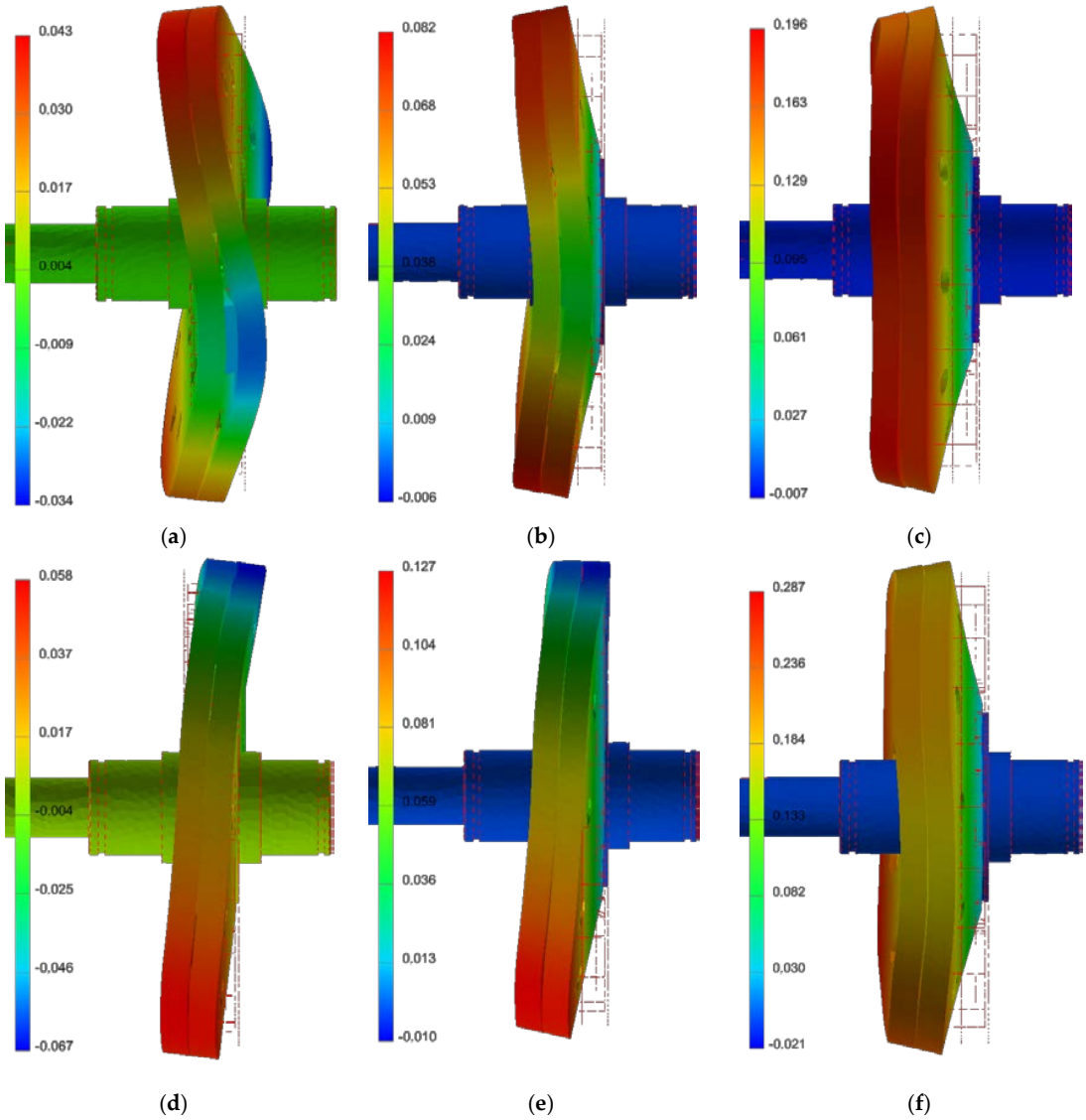

Figure 14. Results of displacements in the Z axis at a max load for $Ag_{asm} = -0.5$, $Ag_{asm} = 0$, and $Ag_{asm} = +1$ respectively, (**a**–**c**) MG_1, (**d**–**f**) MG_2.

The aspect of the measurement verification of local forces acting on individual cores is very difficult to implement. Its effects can be observed/measured only by the local deformations. A reasonable solution seems to be a computer simulation based on experimentally determined material parameters and the verification of the static torque (Figure 3). During the torque measurements, the authors observed deformations of greater value compared to the simulation. The authors see a potential cause of increased deformation in the reaction of the system to a change in the air gap. Mechanical analysis based on the given force distribution resulting from the load returns the deformation in response. The deformation of the modulator, in turn, influences the change in the position of the cores, and consequently influences the input value. The system will thus stabilize at another point, and this point/deformation can only be determined by measurement. Therefore, the knowledge gained during the simulation of the reaction of the system can indicate potential threats at the design stage, and allow for taking appropriate preventive steps. In addition, the calculations presented in the work do not include the tolerance of components (after assembly of the AFMG), which, also in the authors' opinion, may significantly affect the measurement results.

6. Conclusions

Nowadays, the potential of AF machines is used in many industrial fields. However, despite numerous advantages, AF transducers also have significant disadvantages, namely, axial forces. This paper is one of a few that analyzes the AFMGs in detail in terms of local and global forces. The authors, based on two selected gear variants with integer (MG_1) and fractional (MG_2) ratios, have presented important features of both structures, focusing on the comparison of torques and forces. The original analysis of forces in AFMGs, including the determination of the MG_2 variant over the MG_1 one, is the main achievement of this paper. The most important advantages of the proposed approach are as follows:

- A holistic view of the problem of stress distribution in the AFMG modulator, locally and globally, as other authors usually present a global approach;
- Detailed analysis of the individual force components of each core, important in the context of the strength and design of the modulator disc (practically unheard of in other works);
- Determination of the influence of the gear ratio (integer/fractional) on the deformation form of the AFMG modulator (Figure 14) (only an example of the structural analysis of the RFMG transmission has been found in the literature);
- Introduction and analysis of variants of air gap asymmetry in the context of the reduction of global values of the axial force component, which has not been found in the literature.

The comparison of torque characteristics indicates, as early as the initial stage, a potentially much better variant of the gear, that is, MG_2. The natural tendency to symmetrize the magnetic circuit may, in some cases, lead to a significant deterioration of the movement parameters of the transducer (MG_1). The effects of using the fractional gear ratio in MG_2 have resulted in the appearance of a RUMF of negligible value and a compensating nature for the centrifugal force. Such kinds of interactions do not significantly affect the deterioration of the modulator working conditions, and can even stabilize its operation.

Of course, the most important operating state is the synchronous operation. The spectral characteristics of the local force components associated with each of the modulator pole pieces are very similar. Thus, the key issue is not only the quantification of local forces (almost identical for both variants of the MG), but also a global view taking into account all local interactions. These visible differences in the force amplitudes and pulsation levels for particular force components, when translated to the global characteristics of Figure 9, also emphasize the advantage of the MG_2 gear variant.

Despite numerous differences, both AFMG variants are characterized by a relatively high value of the AUMF. An effective way to reduce the axial force is proposed. The presented considerations show that by using asymmetric air gaps in both AFMG variants, it is possible to almost completely eliminate the global AUMF, with a slight decrease in the transmitted torque. In addition, the use of air gaps of different thickness may facilitate encapsulation in some applications.

The tools of structural analysis have been employed to assess the use of additive manufacturing in the construction of AFMGs. The use of the asymmetry of air gaps (Figure 14) also allows one to limit the possible deformations caused by the 3D printing of the modulator disc. At the same time, using an example of extreme air gaps asymmetry, it has also been shown that prototyping AFMGs using additive manufacturing is subject to much greater limitations than in the case of the RFMGs variants.

Future research will be focused on the minimization problem for the axial forces, and the maximization of the transmitted torque of the magnetic gears.

Author Contributions: Conceptualization, M.K., J.K. and P.M.; methodology, M.K., J.K. and P.M.; software, R.G.; validation, M.K. and J.K.; investigation, M.K., J.K. and P.M.; resources, M.Ł.; data curation, M.K.; Writing—original draft preparation, J.K.; Writing—review and editing, P.M. and M.Ł.; visualization, M.K., J.K. and R.G.; supervision, M.K. and J.K.; project administration, M.K. and J.K., All authors have read and agreed to the published version of the manuscript.

Funding: This research received no external funding.

Conflicts of Interest: The authors declare no conflict of interest.

References

1. Atallah, K.; Howe, D. A novel high-performance magnetic gear. *IEEE Trans. Magn.* **2001**, *37*, 2844–2846. [CrossRef]
2. Atallah, K.; Calverley, S.; Howe, D. Design, analysis and realisation of a high-performance magnetic gear. *IEE Proc. Electr. Power Appl.* **2004**, *151*, 135–143. [CrossRef]
3. Mezani, S.; Atallah, K.; Howe, D. A high-performance axial-field magnetic gear. *J. Appl. Phys.* **2006**, *99*, 08R303-1–08R303-3. [CrossRef]
4. Lubin, T.; Mezani, S.; Rezzoug, A. Development of a 2-D Analytical Model for the Electromagnetic Computation of Axial-Field Magnetic Gears. *IEEE Trans. Magn.* **2013**, *49*, 5507–5521. [CrossRef]
5. Johnson, M.; Shapoury, A.; Boghrat, P.; Post, M.; Toliyat, H.A. Analysis and development of an axial flux magnetic gear. In Proceedings of the IEEE Energy Conversion Congress and Exposition, Pittsburgh, PA, USA, 14–18 September 2014; pp. 5893–5900. [CrossRef]
6. Johnson, M.; Gardner, M.C.; Toliyat, H.A. Design and analysis of an axial flux magnetically geared generator. In Proceedings of the IEEE Energy Conversion Congress and Exposition, Montreal, QC, Canada, 20–24 September 2015; pp. 6511–6518. [CrossRef]
7. Acharya, V.M.; Bird, J.Z.; Calvin, M. A Flux Focusing Axial Magnetic Gear. *IEEE Trans. Magn.* **2013**, *49*, 4092–4095. [CrossRef]
8. Johnson, M.; Gardner, M.C.; Toliyat, H.A. Analysis of axial field magnetic gears with Halbach arrays. In Proceedings of the IEEE International Electric Machines & Drives Conference, Coeur d'Alene, ID, USA, 10–13 May 2015; pp. 108–114. [CrossRef]
9. Tsai, M.; Ku, L. 3-D Printing-Based Design of Axial Flux Magnetic Gear for High Torque Density. *IEEE Trans. Magn.* **2015**, *51*, 1–4, Art no. 8002704. [CrossRef]
10. Gardner, M.C.; Johnson, M.; Toliyat, H.A. Comparison of Surface Permanent Magnet Axial and Radial Flux Coaxial Magnetic Gears. *IEEE Trans. Energy Convers.* **2018**, *33*, 2250–2259. [CrossRef]
11. Chen, Y.; Fu, W.N.; Ho, S.L.; Liu, H. A Quantitative Comparison Analysis of Radial-Flux, Transverse-Flux, and Axial-Flux Magnetic Gears. *IEEE Trans. Magn.* **2014**, *50*, 1–4, Art no. 8104604. [CrossRef]
12. Andriollo, M.; Graziottin, F.; Tortella, A. Design of an Axial-Type Magnetic Gear for the Contact-Less Recharging of a Heavy-Duty Bus Flywheel Storage System. *IEEE Trans. Ind. Appl.* **2017**, *53*, 3476–3484. [CrossRef]
13. Deng, W.; Zuo, S. Axial Force and Vibroacoustic Analysis of External-Rotor Axial-Flux Motors. *IEEE Trans. Ind. Electron.* **2018**, *65*. [CrossRef]
14. Kang, C.H.; Kang, K.J.; Song, J.Y.; Cho, Y.J.; Jang, G.H. Axial Unbalanced Magnetic Force in a Permanent Magnet Motor Due to a Skewed Magnet and Rotor Eccentricities. *IEEE Trans. Magn.* **2017**, *53*. [CrossRef]
15. Ueno, S.; Mameda, J.; Jiang, C. Analysis and control of radial force and tilt moment for an axial-gap self-bearing motor. In Proceedings of the 2017 IEEE International Electric Machines and Drives Conference, Miami, FL, USA, 21–24 May 2017. [CrossRef]
16. Huang, H.; Bird, J.Z.; Vera, A.L.; Qu, R. An Axial Cycloidal Magnetic Gear That Minimizes the Unbalanced Radial Force. *IEEE Trans. Magn.* **2020**, *56*. [CrossRef]
17. Huang, H.; Qu, R.; Bird, J. Performance of Halbach Cycloidal Magnetic Gears with Respect to Torque Density and Gear Ratio. In Proceedings of the IEEE International Electric Machines Drives Conference, San Diego, CA, USA, 12–15 May 2019; pp. 1977–1984. [CrossRef]
18. Davey, K.; McDonald, L.; Hutson, T. Axial Flux Cycloidal Magnetic Gears. *IEEE Trans. Magn.* **2014**, *50*. [CrossRef]
19. Uppalapati, K.K.; Bird, J.Z. An Iterative Magnetomechanical Deflection Model for a Magnetic Gear. *IEEE Trans. Magn.* **2014**, *50*, 245–248. [CrossRef]
20. Fernando, N.; Saha, S. Torsional shear stress minimization techniques and implications on electromagnetic performance of flux-modulated double rotors. *IEEE Trans. Energy Convers.* **2018**, *33*, 49–58. [CrossRef]
21. Kowol, M.; Kołodziej, J.; Gabor, R.; Łukaniszyn, M.; Jagieła, M. On-Load Characteristics of Local and Global Forces in Co-Axial Magnetic Gear with Reference to Additively Manufactured Parts of Modulator. *Energies* **2020**, *13*, 3169. [CrossRef]
22. Kowol, M.; Kołodziej, J.; Jagieła, M.; Łukaniszyn, M. Impact of Modulator Designs and Materials on Efficiency and Losses in Radial Passive Magnetic Gear. *IEEE Trans. Energy Convers.* **2019**, *34*, 147–154. [CrossRef]
23. Kowol, M.; Kołodziej, J.; Łukaniszyn, M. Application of a genetic algorithm for design optimization of a passive magnetic gear. *Comput. Appl. Electr. Eng.* **2016**, *14*, 220–230.
24. Gerber, S.; Wang, R. Analysis of the end-effects in magnetic gears and magnetically geared machines. In Proceedings of the International Conference on Electrical Machines, Berlin, Germany, 2–5 September 2014; pp. 396–402. [CrossRef]
25. Jian, L.; Deng, Z.; Shi, Y.; Wei, J.; Chan, C.C. The Mechanism How Coaxial Magnetic Gear Transmits Magnetic Torques Between Its Two Rotors: Detailed Analysis of Torque Distribution on Modulating Ring. *IEEE/ASME Trans. Mechatron.* **2019**, *24*, 763–773. [CrossRef]
26. Agenbach, C.J.; Els, D.N.J.; Wang, R.; Gerber, S. Force and Vibration Analysis of Magnetic Gears. In Proceedings of the XIII International Conference on Electrical Machines, Alexandroupoli, Greece, 3–6 September 2018; pp. 752–758. [CrossRef]
27. Hoganas. *Somaloy 3P, Material Data*; Hoganas: Hoganas, Sweden, 2018.